15th Seminar "New Trends in Research of Energetic Materials", Part II, pp. 866-880, ISBN 978-80-7395-480-2, University of Pardubice, Pardubice, Czech Republic, April 18–20, 2012.

Research of influence of nozzle geometry on internal ballistics performances of solid propellant rocket motors using numerical simulations

Jasmin Terzic, Berko Zecevic, Sabina Serdarevic-Kadic, Alan Catovic, Mario Baskarad

University of Sarajevo, Mechanical Engineering Faculty, Sarajevo, Bosnia and Herzegovina

terzic@mef.unsa.ba

Abstract:

For tactical rocket motors with more nozzles allocated in a certain spatial distance from the nozzle axis, the products of combustion after the exit from internal cavity of propellant grain do not enter immediately into the nozzle. Products of combustion are reflected of the nozzle wall, swirling flow in front of the nozzle emerges, and only then products of combustion enter into convergent-divergent conical nozzles. There is a significant change in velocity vector and pressure redistribution of gas flow in region ahead of the nozzle, which bring about changes in development of pressure in rocket motor and change of internal ballistics parameters, such as total and specific impulse of rocket motor.

A better understanding of complexity of gas flow in these cases is possible using numerical simulation. Research was focused to analysis of flow of double base propellant combustion products (without metal particles in rocket motors), and the influence of shape of the channel for passage of gases and region in front of nozzle and nozzle geometry to distribution of pressure and flow of the gasses inside rocket motor. For simulation of real gas flow through channel for passage of gases and nozzle, CFD package Comet was used. Using numerical simulations, energy losses in the channels for passage of gases and in front of the nozzle were estimated.

Correlations of individual influences and losses were included in program SPPMEF (authors model for prediction of internal ballistics parameters of rocket motors), enabling more realistic prediction of internal ballistics performance of rocket motors.

Keywords: rocket motors; numerical simulation; central convergent-divergent nozzle; multiple peripheral nozzles; performance;

1 Introduction

Most of the tactical solid propellant rocket motors are designed to use single central nozzle or multiple nozzles that can be arranged around periphery of nozzle block, with axis of symmetry parallel to rocket motor axis of symmetry or under some spatial angle

For tactical rocket motors with multiple nozzles spatially distributed at some distance from nozzle axis, combustion products does not enter into nozzle immediately after exiting the internal propellant grain cavity. Combustion products reflect of nozzle wall, complex vortex flow appears in frontal region of the nozzle followed by combustion products entering into convergent-divergent cone nozzles. Significant changes of gas flow velocity vector and distribution of gas flow pressure in this region emerge which reflects on changes of pressure inside rocket motor and internal ballistics parameters, such as total and specific impulse of rocket motor [1].

Combustion pressure in starting phase of steady combustion process is significantly greater for motor with peripherally distributed nozzles (case with and without erosion of critical nozzle section) compared to rocket motor with central nozzle (fig. 1)

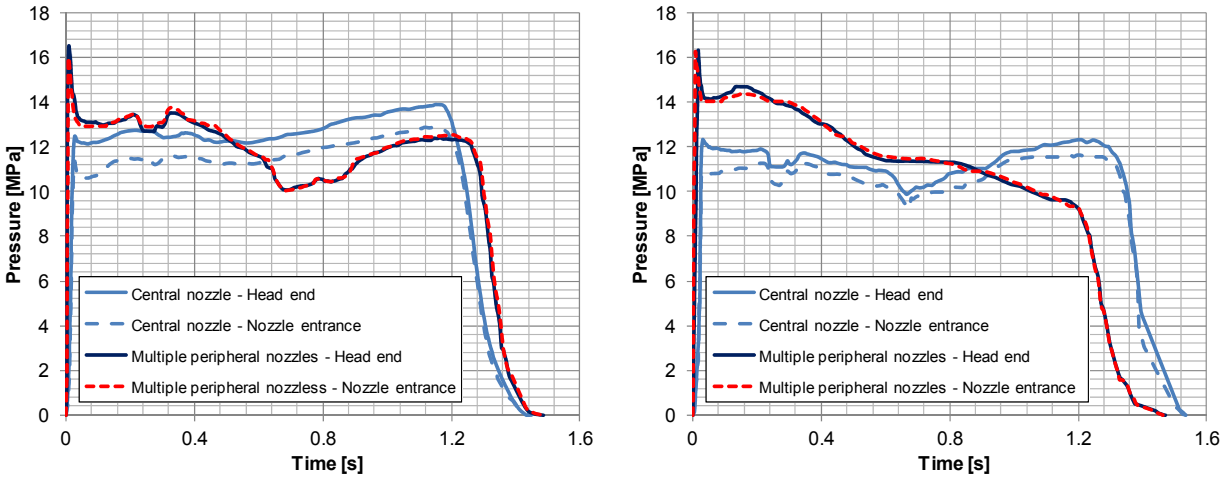

Figure 1: Influence of nozzle type on development of curve pressure-time without erosion (left) and with erosion of nozzle critical section (right)

This increase of pressure influences burning rate and working time of rocket motor, particularly in the case of erosion of nozzle critical section.

Gas flow becomes even more complex for rocket motor rotating around symmetry axis (nozzles inclined at some angle to rocket motor main axis) [1].

Understanding of complexity of gas flow in these cases is possible only by using methods of numerical simulation.

2 Research methods

Investigation of nozzle geometry influence on internal ballistics parameters of solid propellant rocket motors was conducted using numerical simulation methods and analysis of results from experimental testing of rocket motors, in order to assess energetic losses inside rocket motor with central convergent-divergent nozzle and for peripherally distributed nozzles.

Main focus of research was analysis of flow of double base propellant (no metallic particles) combustion products inside rocket motor up to critical section of nozzle (divergent section of nozzle does not influences on processes inside rocket motor), and influence of nozzle region and region in front of the nozzle on gas flow pressure and velocity distribution inside rocket motor for internal burning tube grain.

2.1 Experimental rocket motors

For assessment of internal ballistics parameters of solid propellant rocket motors real experimental rocket motors with nozzle were used, with and without erosion of nozzle critical section:

- Experimental rocket motor with 128 mm diameter, designated as RM-3, contained star propellant grain and central nozzle made from steel without erosion (graphite segment in critical section) and with erosion (steel segment inside critical section) of critical nozzle section (fig. 2).
- Experimental rocket motor with 128 mm diameter, designated as RM-4, contained star propellant grain and nozzle with eight peripherally distributed nozzles. First group of these motors was made with graphite segment in critical section (RM-42) and second group with steel segment inside critical section (RM-41) (fig. 3).
- Experimental motor RM-5 has the same dimensions as previous rocket motor but with internal burning tube grain, with peripherally distributed nozzles and erosion of critical section. First group of motors was made with eight peripherally distributed nozzles (RM-51)

and second group with seven peripherally distributed nozzles with same dimensions as previous (RM-52).

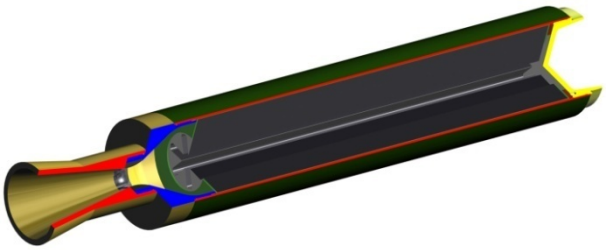

Figure 2: Experimental rocket motor RM-3

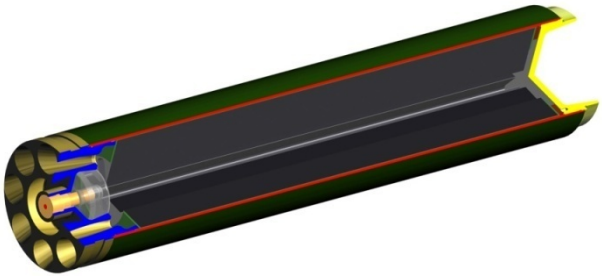

Figure 3: Experimental rocket motor RM-4

In order to investigate individual influences of nozzle geometry on internal ballistics parameters of rocket motors, numerical simulation was conducted, using software package *Comet* [2] based on model presented in reference [3].

Because of complexity of an influence of a section of the rocket motor in front of the nozzle (convergent section of nozzle, peripheral nozzle) on gas flow in rocket motor it was necessary to:

- Assess the influence of convergent section of the nozzle on changes in internal ballistics parameters of rocket motors with central nozzle.
- Assess the influence of peripheral nozzles on performances in rocket motor, compared to central nozzle.
- Established correlations of influence of shape and type of nozzle on change of combustion pressure and losses of specific impulse of rocket motor need to be implemented in the model of program SPPMEF [4,6]. Then the results of prediction of influence of nozzle shape on performances are compared to results of testing of rocket motor with internal burning tube grain (RM-5) and star grain (RM-4)

2.2 Influence of convergent section of nozzle on internal ballistics parameters of rocket motor with central nozzle

For assessment of influence of geometry of convergent section of central nozzle on internal ballistics parameters of rocket motor, numerical simulation for two types of rocket motors was conducted:

- First type of motor was based on concept of motor 32/16 with internal-external burning tube grain.
- Second type of rocket motor was based on the concept of test rocket motor RM-5, designation RM-5_1.

In the simulation geometry of propellant grain did not change, as well as dimension of rocket motor chambers. Only change of convergent section of nozzle was done for following cases of angle of convergency: 45° (standard angle for both types of rocket motors), 60°, 75° and 90°. Radius at the inlet of critical section of nozzle for all simulated angles and for all types of rocket motors remained the same. Dimensions of critical section and divergent section of nozzle remained the same (fig. 4 and 5).

Simulation of internal ballistics parameters for both types of rocket motor was conducted for rocket propellant NGR-A, with characteristics of combustion products determined for nominal combustion pressure, based on program *TCPSP* [4,5] (table 1).

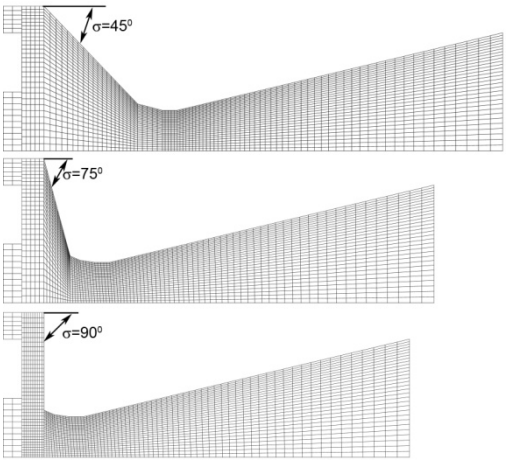

Figure 4: Geometries of central convergent-divergent nozzle for rocket motor 32/16

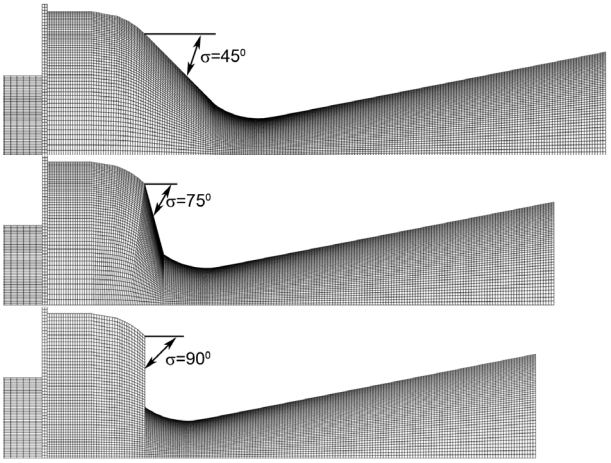

Figure 5: Geometries of central convergent-divergent nozzle for rocket motor RM-5_1

Table 1: Characteristics of rocket motors and propellants NGR-A

Type of rocket motors	32/16	128 mm
Length of combustion chamber, mm	133	526.5
Diameter of combustion chamber, mm	39.2	119.8
Diameter of propellant grain, mm	32	119.8
Internal diameter of propellant grain, mm	16	63.3
Length of propellant grain, mm	125	500
Diameter of throat area, mm	11	29.4
The nozzle-divergence half-angle	13°	11°
Density of propellant, kg/m^3	1600	
Specific heat of propellant, J/(kg K)	1450	
Temperature of combustion, K	2351.0	
Temperature of burning surface, K	650	
Burning rate law, m/s	$0.0130717[p(\text{MPa})]^{0.227587}$ for p_c<14MPa, $0.02161558[p(\text{MPa})]^{0.036981}$	
Specific heat of gasses, J/(kg K)	1814.2	
Gas constant, J/(kg K)	344.	
Thermal conductivity, W/mK	0.1853	
The molar mass, g/mol	24.183	
The ratio of specific heat	1.2463	

Change of pressure as a function of time for rocket motor 32/16 is shown on figure 6a) and for rocket motor RM-5_1 on figure 6b).

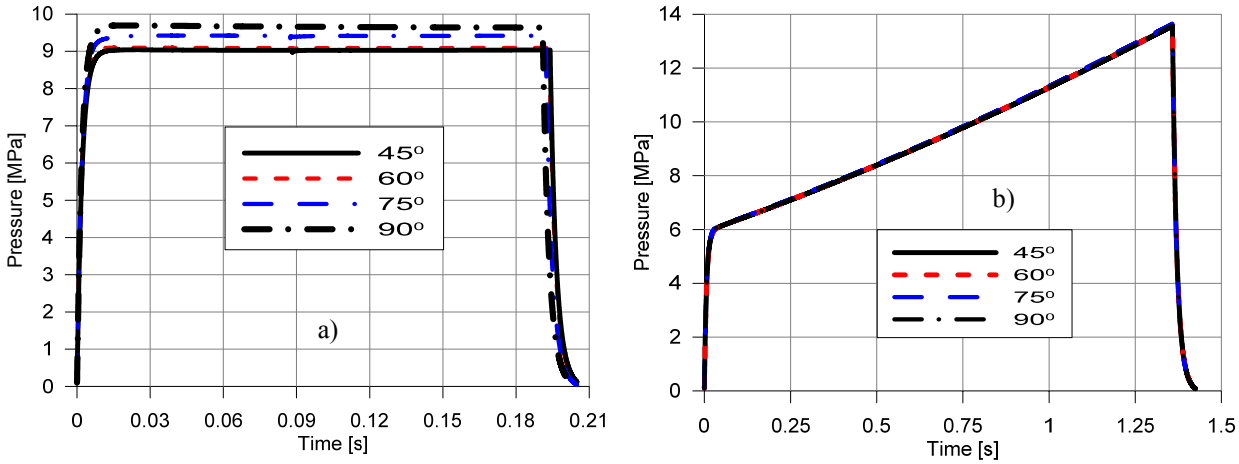

Figure 6: Influence of central nozzle angle on change of pressure as a function of time on head end of rocket motor: a) 32/16 and b) RM-5_1

For rocket motor 32/16 when changing the angle of convergence from 45° to 90°, combustion pressure is increased (fig. 6a). Results of simulation for rocket motor RM-5_1 showed smaller changes of pressure with increase of nozzle angle of convergence (fig. 6b).

For rocket motor 32/16 combustion products from inner channel for passage of gases enter undisturbed into convergent section of nozzle, while combustion products from outer channel for passage of gases hit the wall of convergent section of nozzle and only after that enter into critical nozzle section.

With the increase of angle of convergence, products of combustion from outer channel have greater energy loss, greater reduction in gas velocity (fig. 7a and 7b, 90°) and increase of pressure inside rocket motor compared to inner channel gas flow.

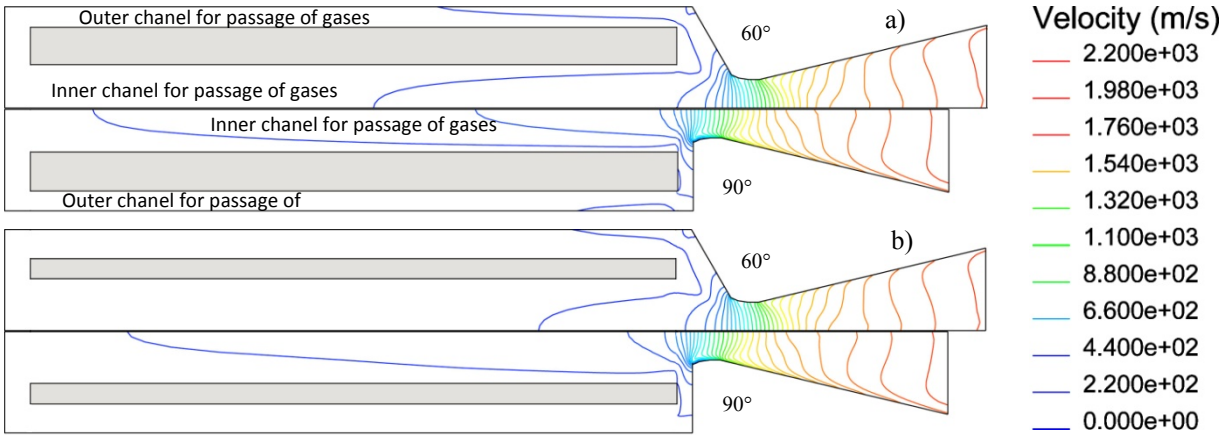

Figure 7: Change of gas velocity inside rocket motor 32/16 for angle of nozzle convergency 60° and 90° in different times of propellant combustion: a) t=19.985ms and b) t= 99.985 ms

With an increase of angle of convergency, increase of gas flow was noticed inside inner channel, which caused greater pressure drop in rocket motor (fig. 8).

Drop of pressure along rocket motor is largest in simulation with nozzle convergency angle 90°. Values of pressure drop are from 4.7% (at the beginning of combustion) to 3.4% (at the end of combustion). For angle of convergency up to 75° this drop is not significant and it is under 1.7%.

For rocket motor RM-5_1, propellant burns only from inner side and combustion products flow from central channel and they don't encounter obstacles and immediately enter into convergent section of nozzle.

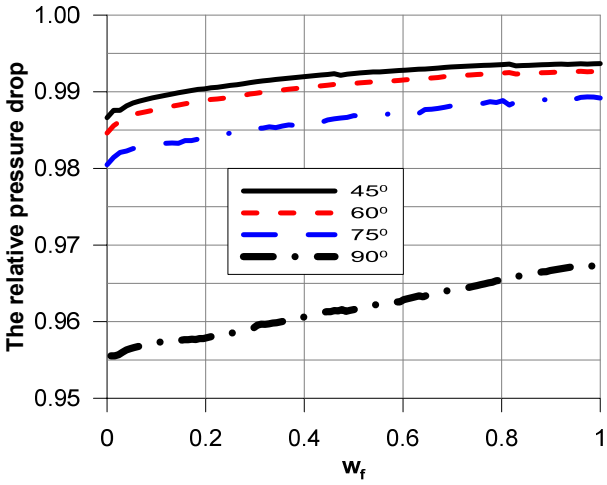

Figure 8: Influence of angle of convergency on relative drop of pressure along motor during combustion process for rocket motor 32/16

Because of small resistance to gas flow, there is no significant change of gas velocity or change of pressure along rocket motor. Change of angle of convergency does not influence pressure drop along rocket motor as in the case of internal-external burning tube grain.

Ratio of length of front end of propellant grain and front part of convergent nozzle to internal diameter of combustion chamber ($L_{P\text{-}ZM}/D$) for rocket motor RM-5_1 is 0.18, and for rocket motor 32/16 this ratio is 0.077. Influence of this distance on pressure change in time is simulated in rocket motor 32/16 for case of nozzle convergency angle of 90°. Results showed that this distance influences only pressure drop along rocket motor. In this case of simulation ($L_{P\text{-}ZM}/D$=0.18) pressure drop along motor is at level of angles under 75° and it is around 1%.

2.2.1 Influence on pressure-time integral

Total influence of angle of convergency on change of pressure-time integral for both types of rocket motor is predicted from ratio:

$$k_\sigma = \frac{\int_0^{t_{tot}} p_c(t,\sigma)\cdot dt}{\int_0^{t_{tot}} p_c(t,\sigma=45^\circ)\cdot dt} \qquad (1)$$

where: $p_c(t,\sigma)$ is pressure in combustion chamber of rocket motor with central nozzle and angle of convergency σ>45° and $p_c(t,\sigma=45^\circ)$ is pressure in combustion chamber of rocket motor with central nozzle and angle of convergency σ=45°.
Character of this influence is shown on figure 9.

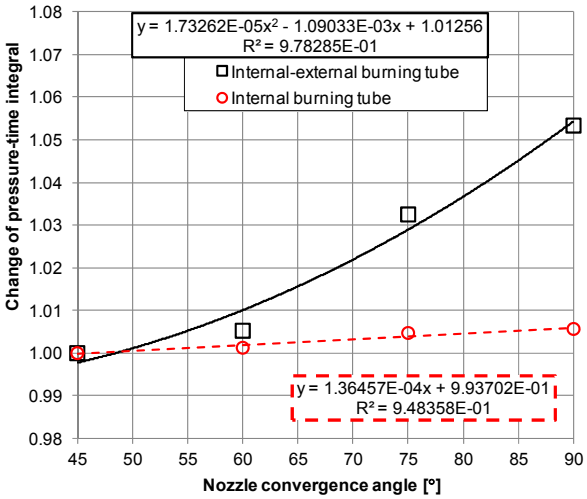

Figure 9: Change of pressure-time integral at the head end of rocket motor with change of nozzle convergency angle

Value of pressure-time integral in rocket motor increases with increase of an angle of convergency for rocket motors where nozzle angle is larger than 45°. This trend is present in both types of rocket motors and both geometries of propellant grain.

Influence of angle of convergency is more pronounced for rocket motor 32/16 that has internal-external burning tube grain.

2.2.2 Specific impulse of rocket motor

Change of degree of efficacy of rocket motor because of change of nozzle angle of convergency for both types of rocket motors is assessed from ratio:

$$\eta_\sigma = \frac{\int_0^{t_{tot}} F(t,\sigma)\cdot dt}{\int_0^{t_{tot}} F(t,\sigma=45^\circ)\cdot dt} \qquad (2)$$

where: $F(t,\sigma)$ is thrust of rocket motor with central nozzle and angle of convergency σ, and $F(t,\sigma=45^\circ)$ is thrust of rocket motor with central nozzle and angle of convergency σ=45°.

Character of this influence is shown on figure 10.

Increase of an angle of convergency decreases specific impulse.

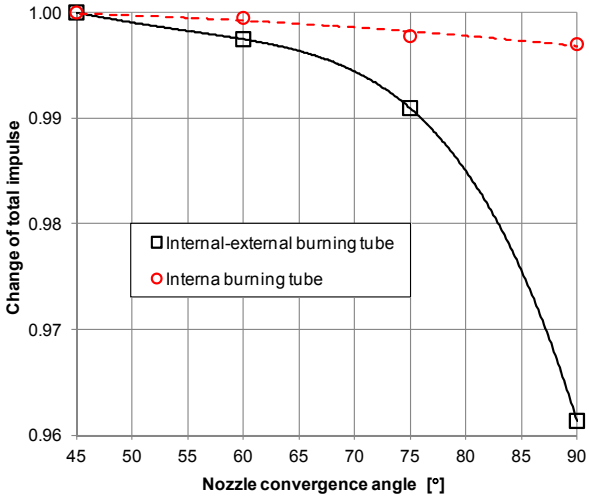

Figure 10: Change of total impulse with change of nozzle angle of convergency

This loss is more pronounced in rocket motors with internal-external burning tube grain than for rocket motors with internal burning tube grain.

By using numerical simulation of rocket motors with propellant NGR-A it was possible to correlate following functions of specific impulse loss with change of angle of convergency:

- for internal-external burning tube grain:

$$\varepsilon_\sigma(\sigma) = 1.25727 \cdot 10^{-6} \cdot \sigma^4 - 2.45200 \cdot 10^{-4} \cdot \sigma^3 + 1.75838 \cdot 10^{-2} \cdot \sigma^2 - 0.530731 \cdot \sigma + 5.46391 \quad \textbf{(3)}$$

- for internal burning tube grain:

$$\varepsilon_\sigma(\sigma) = 8.90194 \cdot 10^{-5} \cdot \sigma^2 - 5.16798 \cdot 10^{-3} \cdot \sigma + 5.85728 \cdot 10^{-2} \quad \textbf{(4)}$$

2.3 Influence of nozzle type on internal ballistics parameters of rocket motors

Simulation of influence of nozzle type on internal ballistics parameters of rocket motors was conducted for two types of rocket motors RM-5, with internal burning tube grain:

- First rocket motor RM-5_2 had central nozzle, and
- Second rocket motor RM-5_3 had nozzle with eight peripherally distributed nozzles.

In simulation both rocket motors were considered as 2D axisymmetric problems with solving domain of 45°. Total surface of nozzle critical section for both motors is the same (no erosion of critical section) and angle of divergence for both motors was 11°. Numerical mesh and spatial domain differed only in section in front of the nozzle and in nozzle region (fig. 11).

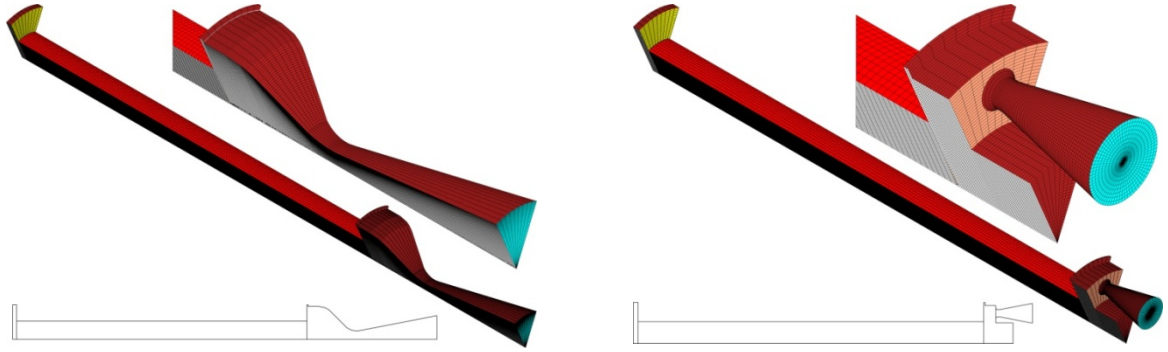

Figure 11: Sl. 6.16 Numerical mesh for rocket motors: a) RM-5_2, b) RM-5_3

Simulation of influence of nozzle type on internal ballistics parameters was performed for six different relative positions of flame front (w_f=w_i/R): 0.0, 0.14159, 0.31858, 0.49558, 0.67257, 1.0. For each relative positions of flame front, values of equilibrium combustion pressure at the head end of rocket motor and in the nozzle entrance (fig. 12) were obtained, as well as pressure value.

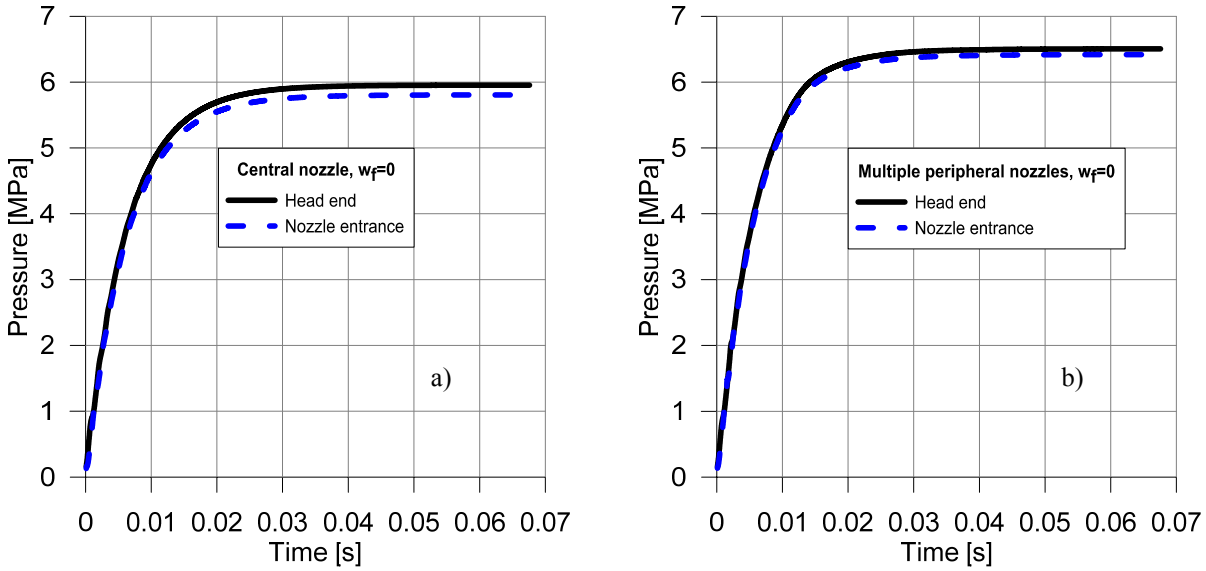

Figure 12: Equilibrium combustion pressure at the head end of rocket motor and in the nozzle entrance for relative position of flame front w_f=0: a) central nozzle b) multiple peripheral nozzles

Figures 12 and 13 show that for rocket motor with peripherally distributed nozzles there is an increase of pressure inside chamber compared to central nozzle. Increase of pressure is specially highlighted in the phase of stable combustion.

Increase of pressure inside rocket motor is a consequence of combustion products from channel for passage of gases do not enter immediately into nozzles but first hit the wall of central section of nozzle, where ignition was positioned, and then they bounce off and enter peripheral part of nozzle. After that combustion products enter nozzle (fig. 14, arrow represent main directions of flow).

When entering nozzle, combustion products have different velocities, and in the nozzle they have asymmetric flow, which is not the case for gas flow through central nozzle.

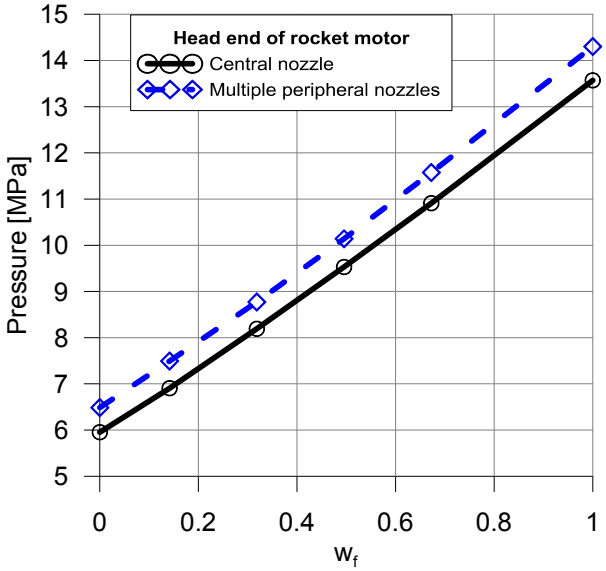

Figure 13: Influence of nozzle type on pressure change at the head end of rocket motor as a function of relative position of flame front

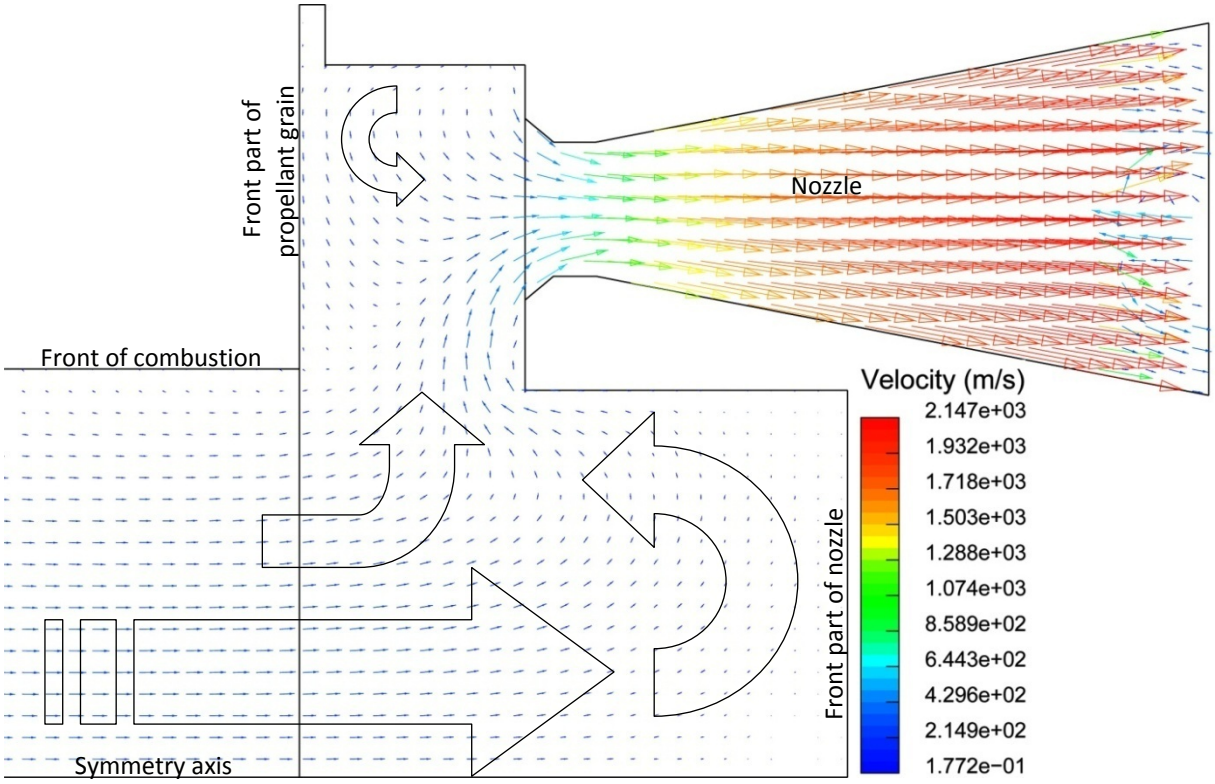

Figure 14: Velocity vector field of gas in frontal part of rocket motor RM-5_3 after t=4.585 ms (p_1=3.4995 MPa, p_2=3.40085 MPa)

During period of establishing stable gas flow, because of complex gas flow in zone in front of the nozzle, there is decrease of gas flow velocity and local oscillations of pressure values in this zone. This process is very short (fig. 15).

After this period there is a period of stable gas flow, and pressure at the end of rocket motor is larger than the pressure in nozzle zone.

By performing simulation of gas flow for rocket motor model with peripherally distributed nozzles, reverse gas flow, reduction of gas flow and increase of local pressure in central zone on nozzle were noticed. With this model of rocket motor smaller decrease of pressure along motor is observed, compared to results of simulation for rocket motor model with central nozzle.

Pressure drop along rocket motor for model with central nozzle is from 2.4% at the beginning of combustion process and up to 1% at the end of combustion process. For model with peripherally distributed nozzles, pressure drop is smaller than 1.3%. These data are in accordance with experimental data for rocket motor RM-4 where pressure drop of around 1% was registered.

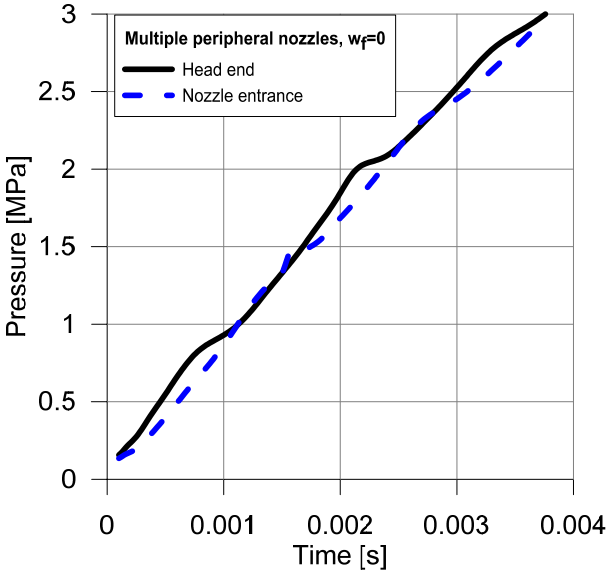

Figure 15: Change of pressure at the head end of rocket motor and in the nozzle entrance in starting phase of work for rocket motor RM-5_3

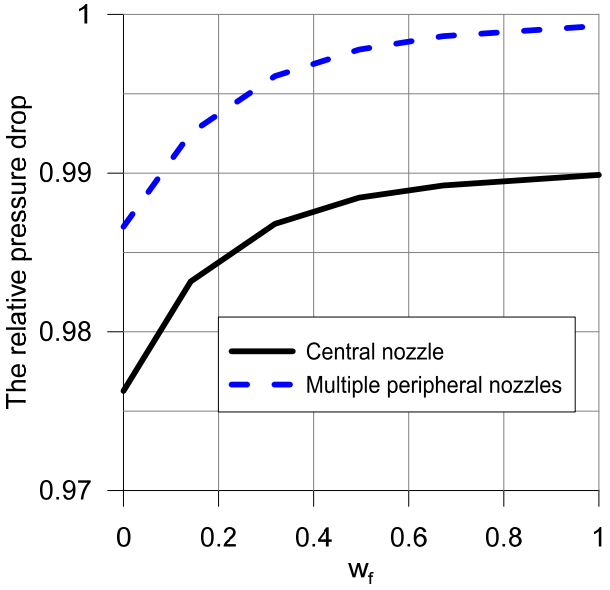

Figure 16: Influence of nozzle type on relative pressure drop along rocket motor during combustion

2.3.1 Influence on instantaneous combustion pressure

In rocket motors with peripherally distributed nozzles, there is significant change of gas flow velocity vector, or gas flow pressure in nozzle entrance region. This influences change of pressure in rocket motor and change of internal ballistics parameters (total and specific impulse of rocket motor)

Total influence of nozzle type on change of instantaneous combustion pressure was obtained from relation:

$$k_{multi} = \frac{p_{c_{multi}}(w_i)}{p_{c_{CM}}(w_i)} \qquad \textbf{(5)}$$

where: $p_{c_{multi}}(w_i)$ – instantaneous combustion pressure of rocket motor with peripherally distributed nozzles and $p_{c_{CM}}(w_i)$ – instantaneous combustion pressure of rocket motor with central nozzle and convergent angle 45°, w_i – location of flame front.

Intensity and character of coefficient of increase of instantaneous pressure of rocket motor with peripherally distributed nozzles as a function of coefficient K_p (ratio of burning surface and area of section of gas passage channel) is shown in figure 17.

Increase of instantaneous pressure is more intensive in the beginning of combustion process (9%) when the area for gas passage in central cavity is smallest (coefficient K_p largest), and decreases with the increase of an area for gas passage in grain (5%).

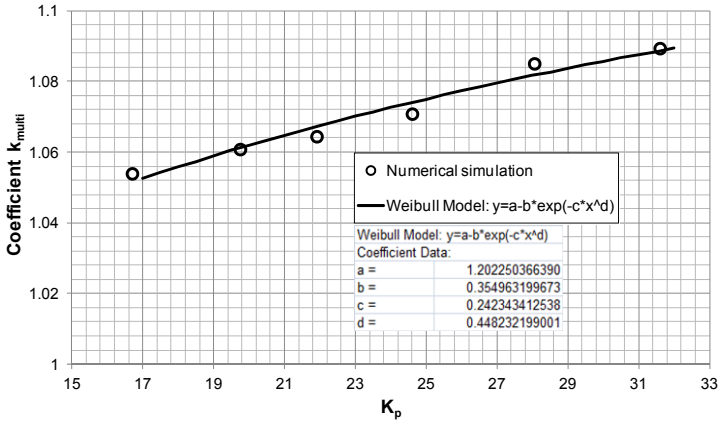

Figure 17: Intensity and character of coefficient of increase of instantaneous pressure of rocket motor with peripherally distributed nozzles as a function of coefficient K_p

Using numerical simulation of rocket motors with propellant NGR-A following dependence of increase of instantaneous pressure in combustion chamber as a function of coefficient K_p is established:

$$k_{multi}(K_p) = 1.2022503664 - 0.3549631997 \cdot e^{\left(-0.24234341254 \cdot K_p^{0.44822199}\right)} \quad \textbf{(6)}$$

2.3.2 Influence on specific impulse

Figure 18 contains diagrams thrust vs time for rocket motors RM-3 and RM-4, obtained with limited experimental research.

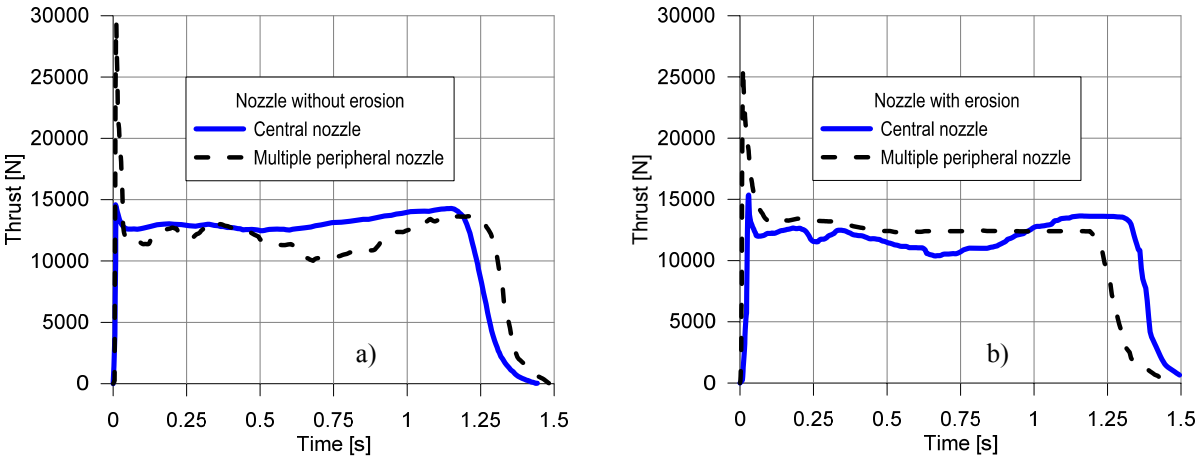

Figure 18: Change of thrust as a function of time for rocket motors RM-3 (central nozzle) and RM-4 (peripheral nozzle): a) no erosion i b) with erosion of nozzle critical section

Type of nozzle influences the changes in specific impulse. For rocket motors with peripherally distributed nozzles we noticed decrease of specific impulse compared to motors with central nozzle. Values of specific impulse loss differ depending on whether there is erosion or there is not erosion of nozzle critical section.

In case of erosion of nozzle critical section, specific impulse loss in rocket motors with peripherally distributed nozzles was 1.1% compared to rocket motors with central nozzle, while for rocket motors with no erosion of nozzle critical section, specific impulse loss was 1.8%.

Numerical simulation of influence of nozzle type on specific impulse of rocket motors with no erosion of nozzle critical section was performed.

For each relative position of flame front, values of pressure were obtained using equation:

$$F = \dot{m}_e \cdot v_e + (p_e - p_a) \cdot A_e \quad \textbf{(7)}$$

where: $\dot{m}_e$ – mass flow rate at the exit of nozzle, v_e – velocity of gas at the exit of nozzle, p_e – static pressure of gas at the exit of nozzle, p_a – ambient pressure and A_e – area of exit section of nozzle.

Specific impulse is determined from ratio of motor thrust and mass velocity of gas at the exit of nozzle:

$$I_{sp} = \frac{F}{\dot{m}_e} \quad or \quad I_{sp} = \frac{\int F \cdot dt}{m_p}. \tag{8}$$

Specific impulse loss of rocket motors with peripherally distributed nozzles compared to rocket motors with central nozzle is determined from equation:

$$\varepsilon_{MULT} = \left(1 - \frac{I_{sp\,mult}}{I_{sp\,centr}}\right) \cdot 100 \tag{9}$$

where: ε_{MULT} - specific impulse loss because of complexity of gas flow for motors with multiple nozzles [%], $I_{sp\,mult}$ - specific impulse of rocket motors with peripherally distributed nozzles i $I_{sp\,centr}$ - specific impulse of rocket motors with central nozzle.

Using numerical simulation method, value of specific impulse loss because of complexity of gas flow for motors with multiple nozzles was determined to be 1.65%. Obtained value of this loss is in good agreement with experimental result for rocket motors RM-3 and RM-4 without erosion of nozzle critical section.

3 Model for prediction of internal ballistic performances of rocket motor with peripheral nozzles

For prediction of internal ballistics performances of rocket motor with peripheral nozzles our own model and *SPPMEF* [4,6] were applied. Only additions to existing model will be presented and those are needed for successful prediction internal ballistics performances of rocket motor with peripheral nozzles.

First modification of program was done in module *NOZZLE* (dimensioning nozzle and estimate of rocket motor performances loss) [4,6]. Prediction of real values of specific impulse of rocket motor is complex task and where knowledge is required for theoretical values of specific impulse of propellant, coefficient of efficiency of combustion process η_{C^*} and thrust coefficient of efficiency η_{C_F} :

$$I_{sp} = I_{sp_{teo}} \cdot \eta_{C^*} \cdot \eta_{C_F} \tag{10}$$

Theoretical value of specific impulse of propellant is determined using program *TCPSP*, while coefficients η_{C^*} and η_{C_F} are determined from experimental data or recommendation of AGARD.

Experimental value of coefficient of efficiency of combustion process is presented by ratio of experimental value of characteristic velocity and theoretical value of characteristic velocity:

$$\eta_{C^*_{\exp}} = \frac{A_t \int p\, dt}{m_p \cdot C^{*0}} \tag{11}$$

where: C^{*0} – theoretical value of characteristic velocity for nominal working pressure from module *TCPSP*, m_p – propellant mass.

Thrust coefficient of efficiency η_{C_F} is determined from equation:

$$\eta_{C_F} = 1 - 0{,}01 \cdot \left(\varepsilon_{DIV} + \varepsilon_{TP} + \varepsilon_{BL} + \varepsilon_{KIN} + \varepsilon_{SUB} + \varepsilon_{EROS} + \varepsilon_{\sigma} + \varepsilon_{ANGL} + \varepsilon_{MULT}\right) \quad \textbf{(12)}$$

where: ε_{DIV} – divergence loss, ε_{TP} – two-phase flow loss, ε_{BL} – boundary layer loss, ε_{KIN} - kinetic loss, ε_{SUB} – submergence loss, ε_{EROS} – nozzle erosion loss, ε_{σ} - loss because of change of nozzle angle of convergence, ε_{ANGL} – loss because of change of geometry of entrance section of nozzle which was influenced by change of nozzle angle related to motor axis, ε_{MULT} – loss because of complexity of gas flow for motors with multiple peripheral nozzles.

Loss of specific impulse because of change of nozzle angle of convergence, for case of central nozzle, is determined from equations (3) or (4) depending on propellant shape and character of combustion. For case of multiple peripherally distributed nozzles this loss is not considered ($\varepsilon_{\sigma} = 0$).

Value of loss because of complexity of gas flow for motors with multiple peripheral nozzles is $\varepsilon_{MULT} = 1{,}65\%$, and for central nozzle this loss is not considered ($\varepsilon_{MULT} = 0$).

Next modifications were performed in module *ROCKET* [4,6]. Change of combustion pressure in rocket motor as a function of time, based on conservation of mass law, does not consider effect of pressure changes because of change of geometry and type of nozzle. To take these effects into considerations we need to modify equation of mass for combustion products through the nozzle:

$$\dot{m}_e = \frac{p_c \cdot A_{th}}{C^* \cdot k_{\sigma} \cdot k_{multi}}. \quad \textbf{(13)}$$

Coefficient k_{σ} for central nozzle case is determined from diagram in fig. 9 (dependence of propellant shape and character of propellant combustion). For rocket motors with peripherally distributed nozzles adopted value for coefficient was $k_{\sigma} = 1$.

Coefficient of increase of instantaneous pressure for rocket motors with peripherally distributed nozzles, k_{multi}, as a function of coefficient K_p, is determined from equation (6), and for central nozzle $k_{multi} = 1$.

Change of combustion pressure in rocket motor, with corrections that take into consideration effects of pressure change because of change of nozzle geometry and type, is determined by numerical integration of following expression:

$$\frac{dp_c}{dt} = \frac{1}{V_{c_i}} \cdot \left[R_g \cdot T_c \cdot \left(\sum_{j=1}^{L/\Delta x} \rho_p \cdot A_{b_{i_j}} \cdot r_{b_{i_j}} - \frac{p_{c_i} \cdot A_{th_i}}{C^* \cdot k_{\sigma} \cdot k_{multi}} \right) - p_{c_i} \cdot \frac{dV_{c_i}}{dt} \right] \quad \textbf{(14)}$$

3.1.1 Verification of new model of program SPPMEF

First phase of verification of corrected model of program SPPMEF was conducted for rocket motors with internal burning tube grain and peripheral nozzles:

- Rocket motor RM-51, eight peripherally distributed nozzles with erosion of nozzle critical section
- Rocket motor RM-52, seven peripherally distributed nozzles with erosion of nozzle critical section.

Second phase of verification of corrected model of program SPPMEF was analysis of influence of changing of propellant grain shape. Rocket motor RM-41 was considered, with star grain and peripherally distributed nozzles with intensive erosion of nozzle critical section

During the process of prediction of internal ballistics parameters for all types of rocket motors, basic burning rate influence on erosive burning (β=120) and HUMP effect were corrected.

Simulation of internal ballistics parameters for all types of rocket motors took into consideration effects of change of instantaneous pressure (equation 6) and additional losses of specific impulse because of change of geometry and nozzle type.

In first case of numerical simulation where change of pressure and thrust as a function of time were considered, rocket motor RM-51 was used. Influence of radial erosion of nozzle critical section was considered with erosion rate of 0.8 mm/s (it was assumed there is no erosion of critical section of nozzle in the process of combustion up to half of the web, and after that more intensive erosion of nozzle critical section occurs [1]).

Figure 19 shows change of pressure, thrust as a function of time for rocket motor RM-51, obtained from program *SPPMEF* and experimental data.

Good agreement was achieved between numerical simulation and experiments.

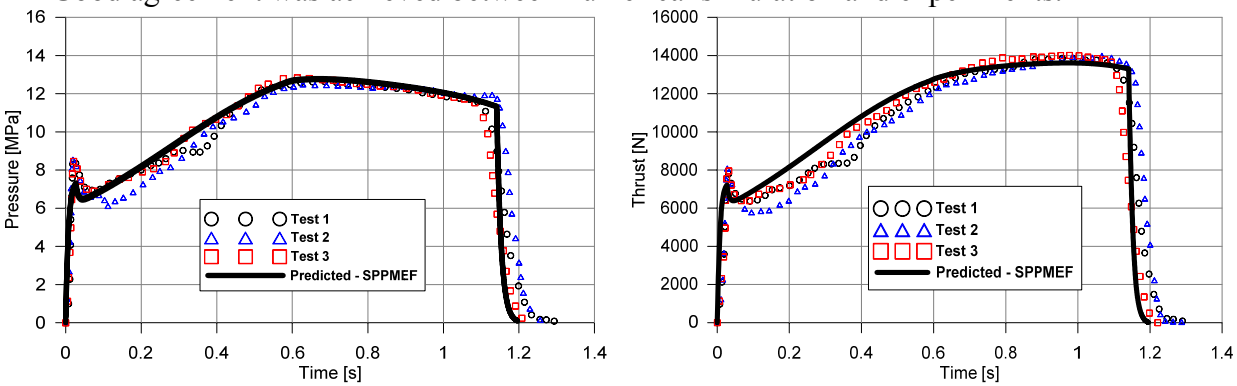

Figure 19: Change of pressure (left) and thrust (right) as a function of time for rocket motor RM-51

Difference in values of integral pressure-time is very small (0.7 %), and difference in maximal pressure is only 1%. Small difference was noticed also for average thrust value (0.12%). Slightly larger differences occur for burning time t_b (1.82%), total impulse and specific impulse (1.95%). These differences could be caused by adopted model of erosion of critical section of peripherally distributed nozzles.

In second case of numerical simulation where change of pressure and thrust as a function of time were considered, rocket motor RM-52 was used. Influence of radial erosion of nozzle critical section was considered with erosion rate of 1.4 mm/s.

Figure 20 shows change of pressure, thrust as a function of time for rocket motor RM-52, obtained from program *SPPMEF* and experimental data.

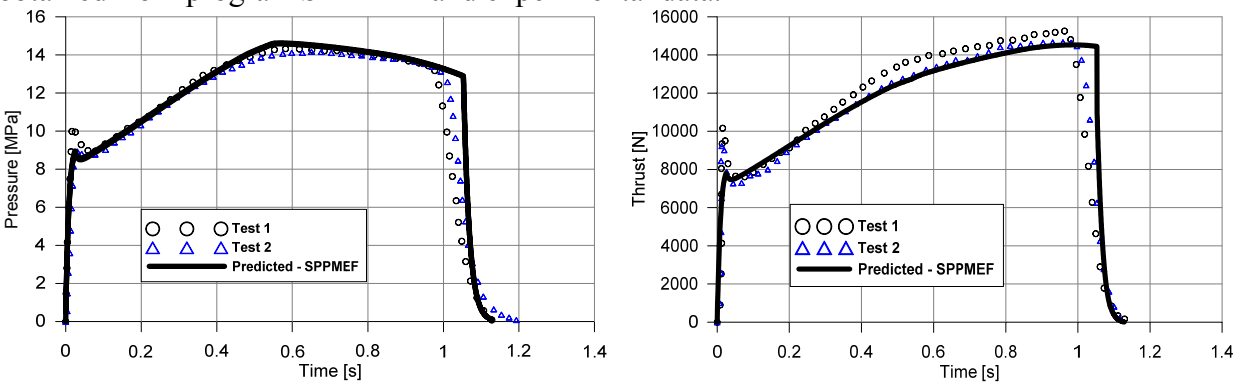

Figure 20: Change of pressure (left) and thrust (right) as a function of time for rocket motor RM-52

Difference in values of integral pressure-time for this motor is slightly larger than for previous motor and it was 3.31 %, and for maximal pressure 2.62%. Larger differences occur for burning time t_b (6.59%) and average thrust (6.07%). Good agreements were obtained for total impulse and specific impulse (0.3%).

For prediction of internal ballistics parameters of rocket motor RM-41 (star grain), model of radial erosion of nozzle critical section was considered with erosion rate of 1.1 mm/s.

Figure 21 shows change of pressure, thrust as a function of time for rocket motor RM-41, obtained from program SPPMEF and experimental data.

Very good agreement was achieved for change of pressure and thrust as a function of time between numerical simulation and experiments.

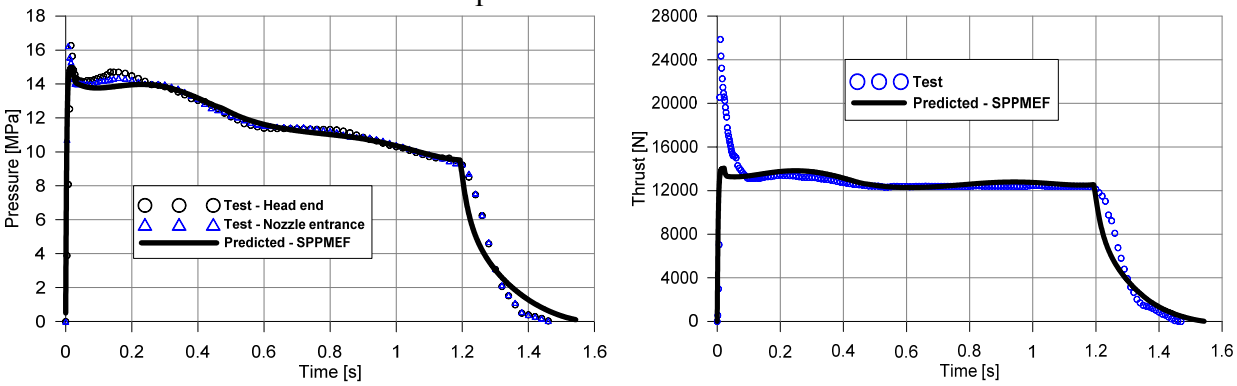

Figure 21: Change of pressure (left) and thrust (right) as a function of time for rocket motor RM-41

Difference in values of total impulse was 0.74%, integral pressure-time up to 0.4%, and specific impulse under 1%, which is very good agreement with experimental test data.

4 Conclusion

Investigation of nozzle geometry influence on internal ballistics parameters of solid propellant rocket motors was conducted using numerical simulation methods and experimental testing of rocket motors, using comparative methods of analysis of obtained results.

As a basic for compilation of results of influence of nozzle geometry on internal ballistics parameters of solid propellant rocket motors we used results of numerical simulation of rocket motors with central nozzle with angle of convergency of 45°.

In assessment of influence of nozzle type on internal ballistics parameters of solid propellant rocket motors, as a basis we used results of numerical simulation of rocket motors with central nozzle.

Intensity of influence of nozzle angle of convergency on value of pressure-time integral depends on propellant grain shape. This influence is more pronounced in rocket motors with internal-external burning tube grain, while the influence is insignificant in rocket motors with internal burning tube grain.

Correlations between changes of specific impulse with change of nozzle angle of convergency as a function of propellant grain shape were obtained.

Increase of nozzle angle of convergency causes decrease of specific impulse. For rocket motors with internal-external burning tube grain this decrease is up to 4 % (nozzle angle of convergency of 90°), and for rocket motors that have with internal burning tube grain decrease of specific impulse is under 0.3%.

Correlation between increases of instantaneous pressure in combustion chamber as a function of coefficient K_p is established for motors with peripheral nozzles. This increase instantaneous pressure is more intensive in the beginning of combustion process when the area for gas passage in central cavity is smallest (coefficient K_p largest), and decreases with the increase of an area for gas passage in grain.

Using numerical simulation we estimated change of specific impulse because of complexity of gas flow for motors with multiple peripheral nozzles, without erosion of nozzle critical section. Change of specific impulse value was 1.65%, which is in accordance with experimental testing.

Comparative analysis of results obtained with prediction (with modified program *SPPMEF*) and data obtained during experimental tests showed:

- Modification of program *SPPMEF* enables successful prediction of performances of rocket motors with peripheral nozzles and internal burning tube grain.
- Very good agreement was achieved for prediction of internal ballistics parameters of solid propellant rocket motors with different number of peripheral nozzles.
- Modification of program *SPPMEF* for internal burning tube grain can be applied for prediction of internal ballistics parameters of solid propellant rocket motors with star grain.

References

[1] B. Zecevic: *Influence of the variable radial acceleration to internal ballistics of rocket motors with DB propellants*, Dissertation, Faculty of Mechanical Engineering, Sarajevo 1999.

[2] *COMET*, ICCM GmbH, Hamburg, Germany, 1997

[3] J. Terzic, B. Zecevic, S. Muzaferija, S. Serdarevic-Kadic, A. Catovic: Numerical simulation of internal ballistics parameters of solid propellant rocket motors, *15th Seminar "New Trends in Research of Energetic Materials"*, University of Pardubice, Pardubice, April 18–20, 2012.

[4] J. Terzic: *Prediction of idealized internal ballistic properties of a rocket motor with DB solid propellant*, Master thesis, University of Sarajevo, Faculty of Mechanical Engineering, Sarajevo, 2002.

[5] J. Terzic, A. Lekic and B. Zecevic: Prediction the Theoretical Interior Ballistic Properties of Solid Propellant Rocket Motors, *6th Seminar "New Trends in Research of Energetic Materials"*, University of Pardubice, pp. 420-435, ISBN 0-7194-543-9 April 2003.

[6] J. Terzic, B. Zecevic, M. Baskarad, A. Catovic, S. Serdarevic-Kadic: Prediction of Internal Ballistic Parameters of Solid Propellant Rocket Motors, *Problems of Mechatronics - Armament, Aviation, Safety Engineering*, 4(6),2011,7-26, ISSN 2081-5891

[7] B. Zecevic, J. Terzić and M. Baskarad: Influence of Solid Propellant Grains Processing on Burning Rate of Double Base Rocket Propellants, *Sixth Seminar "New Trends in Research of Energetic Materials"*, University of Pardubice, Pardubice, pp. 420-435, ISBN 0-7194-543-9, April 2003.